

Preparation, Characterization, and Proton-induced Fluorescence Switching of Two Ru(II) Polypyridyl Complexes containing Different *N*-Heterocyclic Groups

Feixiang Cheng^a, Jishu Chen^a, Fan Wang^a, and Ning Tang^b

^a College of Chemistry and Chemical Engineering, Qujing Normal University, Qujing 655011, P. R. China

^b College of Chemistry and Chemical Engineering, Lanzhou University, Lanzhou 730000, P. R. China

Reprint requests to Dr. Feixiang Cheng. E-mail: chengfx2010@163.com

Z. Naturforsch. **2012**, *67b*, 657–666 / DOI: 10.5560/ZNB.2012-0103

Received April 13, 2012

Two ligands H_2L^1 and HL^2 containing imidazole rings and piperazine or morpholine units have been prepared by the reaction of 1,10-phenanthroline-5,6-dione with 4,4'-(1,4-piperazinediyl)bisbenzaldehyde and 4-morpholinobenzaldehyde, respectively. The Ru(II) polypyridyl complexes $[(bpy)_2Ru(H_2L^1)Ru(bpy)_2]^{4+}$ and $[(bpy)_2Ru(HL^2)]^{2+}$ have been synthesized by the reaction of $Ru(bpy)_2Cl_2 \cdot 2H_2O$ with ligands H_2L^1 and HL^2 , respectively. The pH effects on the UV/Vis absorption and fluorescence spectra of both complexes have been studied. The ground-state and excited-state ionization constants of the acid-base equilibria have been calculated according to the absorbance and emission data. The photophysical properties of both complexes are strongly dependent on the solution pH. They act as proton-induced “off-on-off” fluorescence pH sensors through protonation and deprotonation of the imidazole, piperazine or morpholine groups, with a maximum on-off ratio of 6 in buffer solution at room temperature.

Key words: Ru(II) Complex, pH Switching, UV/Vis Absorption, Fluorescence

Introduction

Luminescent signaling systems that respond to external stimuli which are important for the design of molecular switches and molecular machines have received much attention in recent years [1–4]. Proton-induced luminescent switches are especially appealing for the measurement of pH and pCO_2 in biological, chemical and industrial areas, such as acid rain pollution and environmental monitoring. Various luminescent dyes have been explored for the development of optical pH sensors, including fluorescein, naphthalene, corrole, and coumarin derivatives [5–7]. However, these organic molecules have small Stokes' shifts, overlapping pK_a values and limited photostability. Investigations of luminescent transition metal complexes have attracted less attention, and their great potential as pH sensors has not fully been explored [8–10]. Recently, considerable atten-

tion has been paid to Ru(II) complexes as pH sensors, because their photophysical and electrochemical properties are quite sensitive to external inputs [11, 12]. The general approach for the design of pH-sensitive luminescent metal complexes is to modify a core ligand for pH sensitivity. This concept has been successfully applied to several Ru(II) polypyridyl complexes, and Ru(II) polypyridyl complexes with carboxylic acid, pyridine, amine or phenol groups attached to the core ligands have been reported [13–16]. The choice of ligands is an important factor for a successful pH sensor. Imidazole-containing ligands are poor π acceptors and good π donors compared with pyridine-, pyrazine- and pyrimidine-containing ligands. Furthermore, imidazole-containing ligands possess ionizable N-H protons, which can perturb the electronic properties of their metal complexes through protonation and deprotonation. Although some Ru(II) polypyridyl complexes containing imidazole units have been pre-

pared, in most cases, these complexes are non-emissive or weakly emissive associated with deprotonation processes [17–19]; only those with imidazole units uncoordinated to the Ru(II) centers are good emitters. To the best of our knowledge, only a few mono- and dinuclear Ru(II) polypyridyl complexes of this kind have been reported [20–22]. Similar to most pH indicators, most of the Ru(II) complexes have a narrow pH-sensing range. Therefore, the development of luminescent Ru(II) complexes with a wide-range pH sensing function continues to be an interesting research area. With the aim of preparing Ru(II) complexes covering a broad pH-sensing range, we synthesized two Ru(II) complexes consisting of two different *N*-heterocyclic fragments, each possessing different protonatable/deprotonatable functionalities: imidazole, piperazine, or morpholine. The spectroscopic properties of both complexes in response to pH changes are presented and discussed.

Experimental Section

Materials and physical measurements

2,2'-Bipyridine, 1,10-phenanthroline, 4-fluorobenzaldehyde, piperazine, morpholine, ethylene glycol, RuCl₃·3H₂O, NH₄PF₆, NH₄OAc, CH₃COOH, CH₃CN, EtOH, CH₂Cl₂, and DMF were purchased from the Tianjin Chemical Reagent Factory. Solvents and raw materials were of analytical grade and used as received. An exception was CH₃CN, which was filtered over activated alumina and distilled from P₂O₅ immediately prior to use. 1,10-Phenanthroline-5,6-dione [23], 4,4'-(1,4-piperazinediyl)bisbenzaldehyde [24], 4-morpholinobenzaldehyde [24], and Ru(bpy)₂Cl₂·2H₂O [25] were synthesized according to literature procedures.

¹H NMR spectra were recorded on a Mercury Plus 400 spectrometer using TMS as internal standard. ESI-HRMS spectra were obtained on a Bruker Daltonics APEXII47e mass spectrometer and ESI-TOF spectra with a Mariner Biospectrometry Workstation. Elemental analyses were taken using a Perkin-Elmer 240C analytical instrument. Absorption spectra were obtained on a Varian Cary-100 UV/Vis spectrophotometer and fluorescence spectra with a Hitachi F-4600 spectrophotometer. Electrochemical measurements were carried out at room temperature using a CHI 660B electrochemical workstation. Cyclic voltammetry was performed in CH₃CN and DMF solutions using a micro cell equipped with a platinum disk working electrode, a platinum auxiliary electrode and a saturated potassium chloride calomel reference electrode with 0.1 mol L⁻¹

tetrabutylammonium perchlorate (TBAP) as supporting electrolyte. All samples were purged with nitrogen prior to the measurements.

Synthesis

1,4-Bis(4-(1,10-phenanthroline-[5,6-d]imidazol-2-yl)phenyl)piperazine (H₂L¹)

A mixture of 4,4'-(1,4-piperazinediyl)bisbenzaldehyde (153 mg, 0.52 mmol), 1,10-phenanthroline-5,6-dione (238 mg, 1.13 mmol), and NH₄OAc (1.68 g, 21.82 mol) in glacial acetic acid (20 mL) was heated to 130 °C for 3 h, giving a suspension. The reaction mixture was filtered hot, and the solid was washed successively with EtOH, CH₂Cl₂, DMF, and ethyl ether, affording the desired product as a yellow solid. Yield: 85 mg (24%). No ¹H NMR spectrum was obtained due to its poor solubility in common NMR solvents. – HRMS ((+)-ESI): *m/z* = 675.2742 (calcd. 675.2733 for C₄₂H₃₁N₁₀, [M+H]⁺), 697.2548 (calcd. 697.2553 for C₄₂H₃₀N₉Na, [M+Na]⁺). – Analysis for C₄₂H₃₀N₁₀ (%): calcd. C 74.76, H 4.48, N 20.76; found C 74.91, H 4.61, N 20.62.

4-(4-(1,10-Phenanthroline-[5,6-d]imidazol-2-yl)phenyl)morpholine (HL²)

A mixture of 4-morpholinobenzaldehyde (198 mg, 1.04 mmol), 1,10-phenanthroline-5,6-dione (232 mg, 1.10 mmol), and NH₄OAc (1.62 g, 21.04 mol) in glacial acetic acid (16 mL) was heated to 130 °C for 3 h. The reaction mixture was then cooled to room temperature and poured into water (100 mL). The solution was neutralized with a 28% NH₃ solution, a yellow precipitate was formed and collected by filtration. The precipitate was chromatographed on silica, eluted with EtOH affording the product as a pale-yellow solid. Yield: 148 mg (38%). – ¹H NMR (400 MHz, [D₆]DMSO): δ = 3.23 (t, *J* = 4.4 Hz, 4H), 3.74 (t, *J* = 4.2 Hz, 4H), 7.13 (d, *J* = 8.0 Hz, 2H), 7.80 (dd, *J* = 8.0, 4.2 Hz, 2H), 8.13 (d, *J* = 8.8 Hz, 2H), 8.88 (d, *J* = 8.0 Hz, 2H), 8.99 (d, *J* = 4.0 Hz, 2H), 13.58 (s, 1H). – HRMS ((+)-ESI): *m/z* = 382.1667 (calcd. 382.1668 for C₂₃H₂₀N₅O, [M+H]⁺). – Analysis for C₂₃H₁₉N₅O (%): calcd. C 72.42, H 5.02, N 18.36; found C 72.57, H 5.14, N 18.19.

[(bpy)₂Ru(H₂L¹)Ru(bpy)₂](PF₆)₄[Ru₂(H₂L¹)](PF₆)₄

A mixture of H₂L¹ (75 mg, 0.11 mmol) and Ru(bpy)₂Cl₂·2H₂O (136 mg, 0.26 mmol) in ethylene glycol (20 mL) was heated to 150 °C for 10 h under nitrogen to give a clear deep-red solution. Then the solvent was evaporated under reduced pressure. The residue was purified twice by column chromatography on alumina, eluted first with CH₃CN-EtOH (10 : 1, v/v) to remove

impurities, then with CH₃CN-EtOH (5 : 1, v/v) to afford the complex [(bpy)₂Ru(H₂L¹)Ru(bpy)₂]Cl₄. This complex was dissolved in a minimum amount of water followed by dropwise addition of saturated aqueous NH₄PF₆ until no more precipitate formed. The precipitate was recrystallized from a CH₃CN-Et₂O mixture (vapor diffusion method) to afford a red solid. Yield: 131 mg (56%). – ¹H NMR (400 MHz, [D₆]DMSO): δ = 3.55 (s, 8H), 7.26 (d, *J* = 8.8 Hz, 4H), 7.36 (t, *J* = 6.6 Hz, 4H), 7.58–7.62 (m, 8H), 7.86 (d, *J* = 5.6 Hz, 4H), 7.91 (t, *J* = 6.6 Hz, 4H), 8.04 (d, *J* = 4.8 Hz, 4H), 8.12 (t, *J* = 7.8 Hz, 4H), 8.23 (t, *J* = 7.8 Hz, 4H), 8.33 (d, *J* = 8.0 Hz, 4H), 8.86 (d, *J* = 8.4 Hz, 4H), 8.90 (d, *J* = 8.4 Hz, 4H), 9.08 (t, *J* = 7.8 Hz, 4H). – HRMS ((+)-ESI): *m/z* = 823.1774 [M–3PF₆–H]²⁺, 750.1913 [M–4PF₆–2H]²⁺, 500.4611 [M–4PF₆–H]³⁺. – Analysis for C₈₂H₆₂F₂₄N₅P₄Ru₂ (%): calcd. C 47.32, H 3.00, N 12.11; found C 47.48, H 3.13, N 11.95.

[(bpy)₂Ru(HL²)](PF₆)₂[Ru(HL²)](PF₆)₂

[Ru(HL²)](PF₆)₂ was prepared by the same procedure as described for [Ru₂(H₂L¹)](PF₆)₄, except that HL² (40 mg, 0.10 mmol) was used instead of H₂L¹ to react with Ru(bpy)₂Cl₂·2H₂O (68 mg, 0.13 mmol), and EtOH was used as solvent instead of ethylene glycol. Yield: 87 mg (76%) of a red solid. – ¹H NMR (400 MHz, [D₆]DMSO): δ = 3.75 (t, *J* = 4.4 Hz, 8H), 7.11 (d, *J* = 8.8 Hz, 2H), 7.32 (t, *J* = 6.6 Hz, 2H), 7.57 (t, *J* = 6.6 Hz, 4H), 7.83 (t, *J* = 7.0 Hz, 4H), 7.95 (d, *J* = 4.4 Hz, 2H), 8.08 (t, *J* = 7.8 Hz, 2H), 8.19 (t, *J* = 7.8 Hz, 2H), 8.25 (d, *J* = 8.8 Hz, 2H), 8.83 (d, *J* = 8.4 Hz, 2H), 8.87 (d, *J* = 7.6 Hz, 2H), 9.15 (s, 2H). –

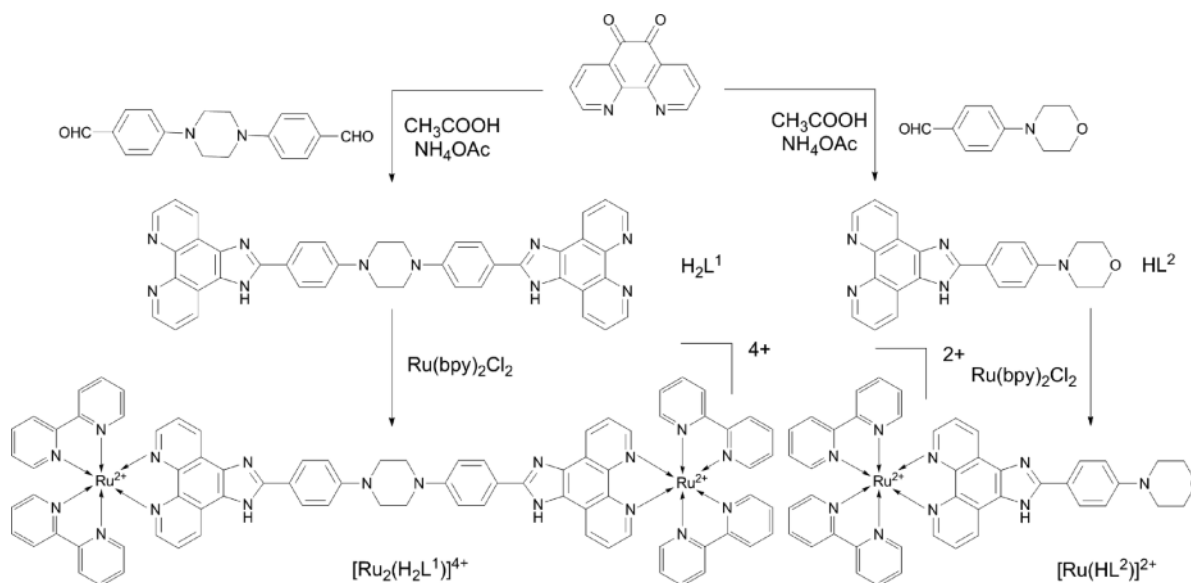
MS (ESI-TOF): *m/z* = 397.6 [M–2PF₆]²⁺. – Analysis for C₄₃H₃₅F₁₂N₉OP₂Ru (%): calcd. C 47.61, H 3.25, N 11.62; found C 47.79, H 3.30, N 11.41.

Results and Discussion

Synthesis and characterization

The outline of the synthesis of the two ligands and their Ru(II) complexes is presented in Scheme 1. The ligands were synthesized on the basis of the method for the imidazole ring preparation established by Steck *et al.* [26]. Ligands H₂L¹ and HL² were synthesized through condensation of 1,10-phenanthroline-5,6-dione with 4,4'-(1,4-piperazinediyl)bisbenzaldehyde and 4-morpholinobenzaldehyde, respectively, in refluxing glacial acetic acid containing ammonium acetate. Both Ru(II) complexes were obtained by refluxing Ru(bpy)₂Cl₂·2H₂O and the ligand in suitable solution, and isolated as PF₆[–] salts in good yields. Both complexes were characterized by elemental analyses, ESI-HRMS, ESI-TOF, and ¹H NMR spectroscopy.

Elemental analyses are well consistent with the formation of both complexes. The structures of both Ru(II) complexes were further established by MS spectra. This technique has proven to be very helpful for identifying transition metal complexes with high molecular masses [27]. The data with the peak assign-



Scheme 1. Synthesis of ligands H₂L¹, HL² and their Ru(II) polypyridyl complexes.

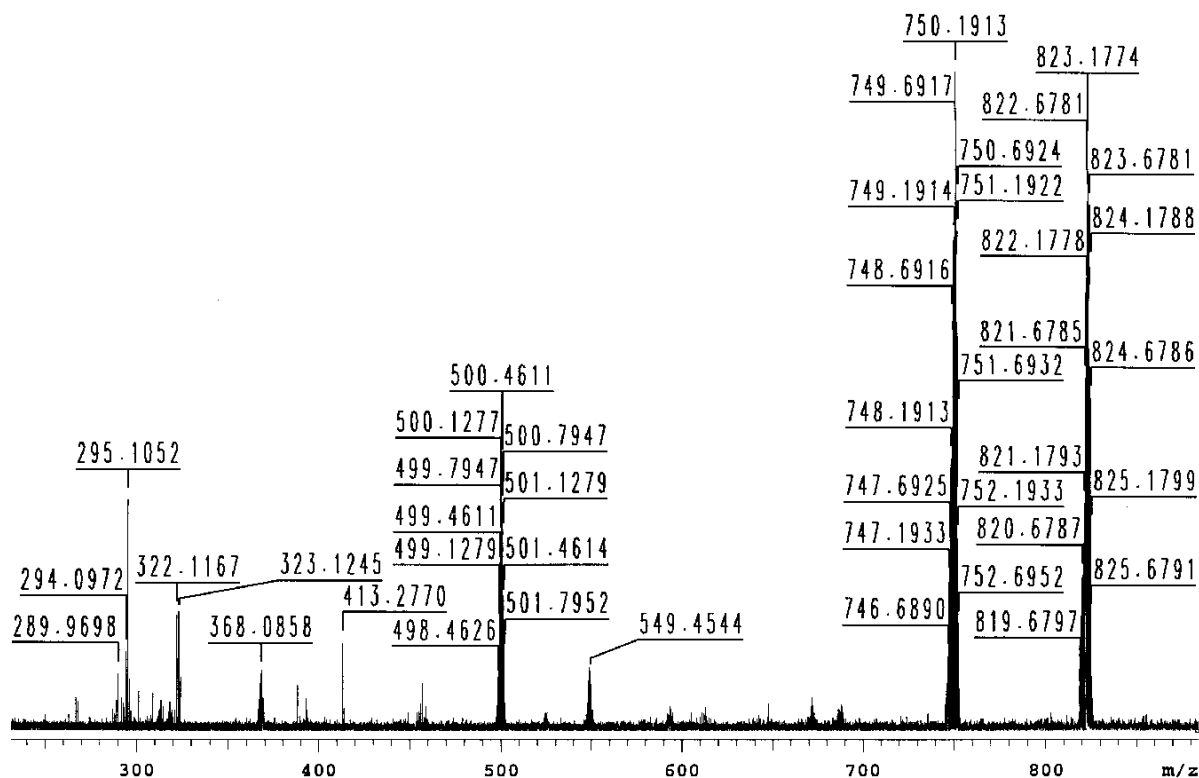


Fig. 1. The ESI-HRMS spectrum of complex $[\text{Ru}_2(\text{H}_2\text{L}^1)](\text{PF}_6)_4$.

ments are given in the Experimental Section. Usually, the mass of Ru(II) polypyridyl complexes with imidazole rings is calculated from a series of multiply-charged ions obtained by the successive loss of counter ions or protons. Fig. 1 shows the ESI-HRMS spectrum of complex $[\text{Ru}_2(\text{H}_2\text{L}^1)](\text{PF}_6)_4$. The main peak at $m/z = 750.1913$ is assigned to $[\text{M}-4\text{PF}_6-2\text{H}]^{2+}$, and the other two peaks at $m/z = 500.4611$ and 823.1774 are assigned to $[\text{M}-3\text{PF}_6-\text{H}]^{2+}$ and 500.4611 $[\text{M}-4\text{PF}_6-\text{H}]^{3+}$, respectively. All the measured ion masses are consistent with the expected values.

Metal centers octahedrally coordinated with bidentate ligands generally show stereoisomerism. A mononuclear octahedral complex can exist in two enantiomeric forms, named Δ and Λ . The dinuclear complex $[\text{Ru}_2(\text{H}_2\text{L}^1)]^{4+}$ can exist in two diastereoisomeric forms, $\Delta\Delta$ (*meso*) and $\Delta\Delta/\Lambda\Lambda$ (*rac*). The ^1H NMR spectra cannot distinguish between the two enantiomers of the mononuclear complex $[\text{Ru}(\text{HL}^2)]^{2+}$. For the dinuclear complex $[\text{Ru}_2(\text{H}_2\text{L}^1)]^{4+}$, the situation is more complicated

due to the existence of diastereoisomers. The down-field region of the ^1H NMR spectra of the complex $[\text{Ru}(\text{HL}^2)]^{2+}$ in $(\text{CD}_3)_2\text{SO}$ solvent is shown in Fig. 2. Two sets of NMR signals are observed, one set corresponds to the ancillary ligand 2,2'-bipyridine, and the other set corresponds to the ligand HL^2 . The chemical shift of the proton on the nitrogen atom of the imidazole group was not observed for the complex $[\text{Ru}(\text{HL}^2)]^{2+}$, since metal coordination causes electron deficiency in the ligand and, as a result, the NH proton is more acidic and easily exchanged between the two nitrogen atoms of the imidazole fragment.

Photophysical properties

The UV/Vis absorption spectra of both complexes were obtained in CH_3CN solution, at a working concentration of $10^{-5} \text{ mol L}^{-1}$. The energy maxima and absorption coefficients are summarized in Table 1, and the spectra are shown in Fig. 3. Assignments of the absorption bands are made on the basis of the well-

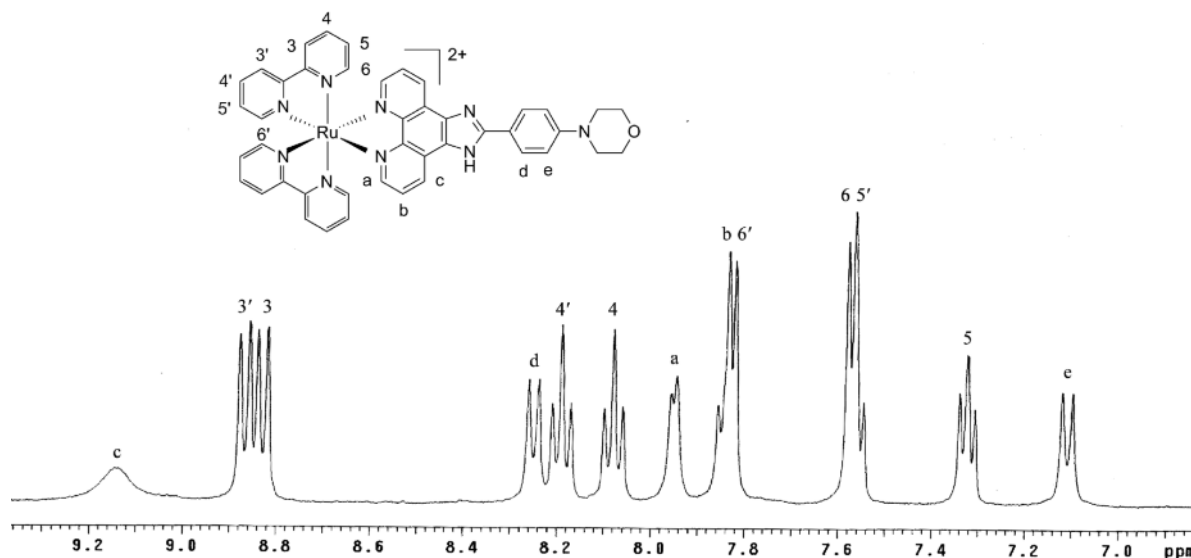


Fig. 2. Downfield region of the ^1H NMR (400 MHz, $[\text{D}_6]\text{DMSO}$) spectrum of complex $[\text{Ru}(\text{HL}^2)]^{2+}$ (Δ and Λ).

Table 1. Photophysical and electrochemical data of the two Ru(II) polypyridyl complexes.

Complex	Absorption	Emission ^a		$E_{1/2}$ (V); ΔE_p (mV) in parentheses ^b	
	λ_{max} (nm); $\epsilon \times 10^4$ ($\text{M}^{-1} \text{cm}^{-1}$) in parentheses	λ_{max} (nm)	Φ	Oxidation	Reduction
$[\text{Ru}_2(\text{H}_2\text{L}^1)]^{4+}$	461 (4.33)	613	0.069	1.31 (80)	-0.90 (86)
	348 (9.44)				-1.31 (96)
	287 (18.82)				-1.53 (69)
	243 (8.21)				
$[\text{Ru}(\text{HL}^2)]^{2+}$	461 (2.44)	613	0.063	1.32 (86)	-0.87 (81)
	341 (5.11)				-1.33 (72)
	287 (11.47)				-1.52 (78)
	243 (4.82)				

^a The uncertainty in quantum yield is 15%; ^b oxidation potentials are recorded in 0.1 mol L^{-1} TBAP/ CH_3CN , reduction potentials are recorded in 0.1 mol L^{-1} TBAP/DMF, and potentials are given vs. SCE; scan rate = 200 mV s^{-1} ; ΔE_p is the difference between the anodic and cathodic waves.

documented optical transitions of analogous Ru(II) polypyridyl complexes [20–22]. The spectra comprise four distinct regions. The bands at around 287 and 243 nm are attributed to intraligand $\pi \rightarrow \pi^*$ transitions centered on the 2,2'-bipyridine. In the higher energy region around 345 nm, the spectra display the characteristic $\pi \rightarrow \pi^*$ band of the core ligand. The band at 461 nm can be assigned to metal-to-ligand charge transfer (MLCT), which consists of overlapping $d\pi(\text{Ru}) \rightarrow \pi^*(\text{bpy})$ and $d\pi(\text{Ru}) \rightarrow \pi^*(\text{L})$ components. The lowered symmetry removes the degeneracy of the π^* levels, which results in the appearance of a non-

symmetrical MLCT band. The MLCT absorption maximum of both complexes is red-shifted by about 11 nm compared with that of $\text{Ru}(\text{bpy})_3^{2+}$ [28] because both ligands have larger π frameworks.

Emission band maxima and emission quantum yields of both complexes are summarized in Table 1. The emission quantum yields are calculated relative to $\text{Ru}(\text{bpy})_3^{2+}$ ($\Phi_{\text{std}} = 0.062$) in deoxygenated CH_3CN [29–31], using the equation $\Phi_{\text{em}} = (\eta_{\text{compd}}^2 / \eta_{\text{std}}^2) (A_{\text{std}} / A_{\text{compd}}) (I_{\text{compd}} / I_{\text{std}}) \Phi_{\text{std}}$. Upon excitation into the MLCT band of both complexes, they show intense emission at around 613 nm

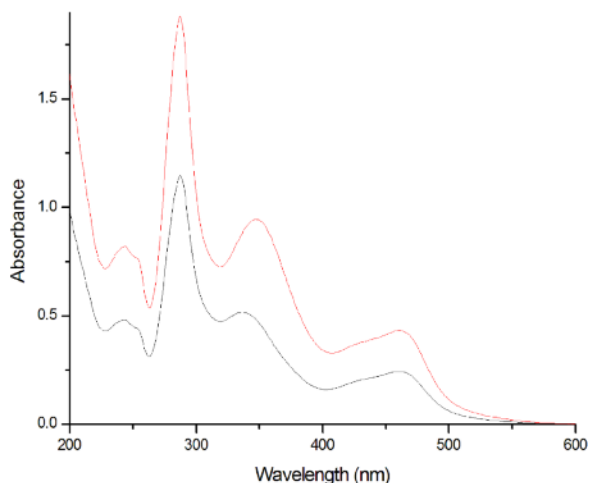


Fig. 3 (color online). Absorption spectra of $[\text{Ru}_2(\text{H}_2\text{L}^1)](\text{PF}_6)_4$ (red) and $[\text{Ru}(\text{HL}^2)](\text{PF}_6)_2$ (black) in CH_3CN at room temperature.

in CH_3CN solution at room temperature, characteristic of the $^3\text{MLCT } d\pi(\text{Ru}) \rightarrow d\pi^*$ emission state.

Electrochemistry

The electrochemical behavior of both complexes was studied in CH_3CN and DMF solutions with 0.1 mol L^{-1} TBAP as supporting electrolyte. In CH_3CN solution, the reductions are not well resolved due to the adsorption of the reduced species onto the surface of the platinum electrode, whereas in DMF, the complexes display three clear reduction processes, but do not show the oxidative waves due to the limitation by the solvent. Therefore, the oxidation potentials were recorded in CH_3CN , but the reduction potentials were recorded in DMF (Table 1).

The complex $[\text{Ru}_2(\text{H}_2\text{L}^1)]^{4+}$ exhibits a Ru(II)-centered oxidation at 1.31 V. This potential is slightly more positive (30 mV) than that of the parent complex $\text{Ru}(\text{bpy})_3^{2+}$ [32], which indicates that the ligand H_2L^1 is a stronger π acceptor than 2,2'-bipyridine. The first reduction of complex $[\text{Ru}_2(\text{H}_2\text{L}^1)]^{4+}$ at -0.90 V shows that this complex is a better electron acceptor than $\text{Ru}(\text{bpy})_3^{2+}$ by about 0.4 V, which is consistent with the addition of electrons to the LUMO orbital localized at the ligand H_2L^1 giving the species $[(\text{bpy})_2\text{Ru}^{\text{II}}\text{H}_2\text{L}^{2-}\text{Ru}^{\text{II}}(\text{bpy})_2]^{2+}$. The second reduction at -1.31 V occurs on one of the two 2,2'-bipyridine ligands of the each Ru(II)

center, thus adding two electrons to the LUMO+1 orbital localized at 2,2'-bipyridine giving the species $[(\text{bpy})(\text{bpy}^{\cdot-})\text{Ru}^{\text{II}}\text{H}_2\text{L}^{2-}\text{Ru}^{\text{II}}(\text{bpy}^{\cdot-})(\text{bpy})]$. The third reduction at -1.53 V affords the species $[(\text{bpy}^{\cdot-})(\text{bpy}^{\cdot-})\text{Ru}^{\text{II}}\text{H}_2\text{L}^{2-}\text{Ru}^{\text{II}}(\text{bpy}^{\cdot-})(\text{bpy}^{\cdot-})]^{2-}$. The electrochemical behavior of complex $[\text{Ru}(\text{HL}^2)]^{2+}$ is similar to that of $[\text{Ru}_2(\text{H}_2\text{L}^1)]^{4+}$.

pH-Dependent photophysical properties

The pH dependence of the ground- and excited-state properties of both complexes has been investigated by UV/Vis absorption and fluorescence spectra, respectively. Spectrophotometric titrations over the pH range 0.03–1.98 were performed in $\text{CH}_3\text{CN}-\text{H}_2\text{O}$ (HClO_4) (1 : 1, v/v) buffer solution, the pH of the solution was adjusted with concentrated aqueous NaOH solution. Spectrophotometric titrations over the pH range 2.05–11.79 were carried out in acetonitrile-Britton-Robinson (1 : 1, v/v) buffer solution with 0.2 mol L^{-1} NaCl to keep a constant ionic strength.

Fig. 4 shows the UV/Vis absorption spectra of complex $[\text{Ru}_2(\text{H}_2\text{L}^1)]^{4+}$ as a function of pH. The spectral changes indicate that the complex undergoes three successive deprotonation processes. Upon increasing the pH from 0.03 to 1.98 (Fig. 4a), the MLCT band at 451 nm and the 2,2'-bipyridine-centered intraligand $\pi \rightarrow \pi^*$ transition band at 283 nm are red-shifted to 456 and 285 nm, respectively, accompanied by slight decreases in their intensities. The bands at 254 and 365 nm are blue-shifted to 245 and 344 nm, respectively, accompanied with decreases in their intensities. The observed spectral changes are attributed to the concurrent dissociation of two protons from the protonated piperazine fragment. The occurrence of one isosbestic point at 336 nm indicates the presence of two species in equilibrium. Several methods can be used to determine the $\text{p}K_a$ values [33–36]; for this work, the spectrophotometric method already reported in the literature for other Ru(II) polypyridyl complexes was chosen [37]. A plot of absorbance at 365 nm *versus* pH for complex $[\text{Ru}_2(\text{H}_2\text{L}^1)]^{4+}$ is given in the inset of Fig. 4a. The pH at the point of inflection gives the value of the first ground-state ionization constant $\text{p}K_{a1}$ of 1.43. The second deprotonation step (Fig. 4b), which takes place over the pH range from 2.05 to 7.19, is assigned to the concurrent dissociation of two protons from the protonated imidazole rings, resulting in the following spectral changes: the absorption intensi-

ties for the bands at 286 and 319 nm become slightly increased, and the minimum at 229 nm decreases in intensity. The value of the second ground-state ionization constant pK_{a2} is 5.59. Further increasing the pH from 7.19 to 11.79 can induce the deprotonation of neutral imidazole groups (Fig. 4c). The bands at 458 and 286 nm are red-shifted to 461 and 288 nm, respectively, accompanied by decreases in their intensities. The band at 319 nm is red-shifted to 329 nm with an obvious increase in intensity. The minimum at 490 nm is increased in intensity with a broader tail extending out to nearly 550 nm. The occurrence of three isosbestic points at 244, 384, and 468 nm indicates the presence of two species in equilibrium.

The value of the third ground-state ionization constant pK_{a3} is 9.06. Three ground-state ionization constants are comparable to previously reported data for analogous Ru(II) complexes. The first ionization constant of the protonated piperazine ring is comparable to the corresponding pK_a value of 1.50 for the complex **1a** [38]. The ionization constant of the protonated imidazole rings is close to the pK_{a2} value of 5.23 for the complex $[\text{Ru}(\text{bpy})_2(\text{Hbopip})]^{2+}$ [39]. The ionization constant of the neutral imidazole rings is comparable to the corresponding value of 9.28 for the complex $[(\text{bpy})_2\text{Ru}(\text{mbpibH}_2)\text{Ru}(\text{bpy})_2]^{4+}$ [40].

The fluorescence spectral changes of the complex $[\text{Ru}_2(\text{H}_2\text{L}^1)]^{4+}$ as a function of pH is shown in Fig. 5.

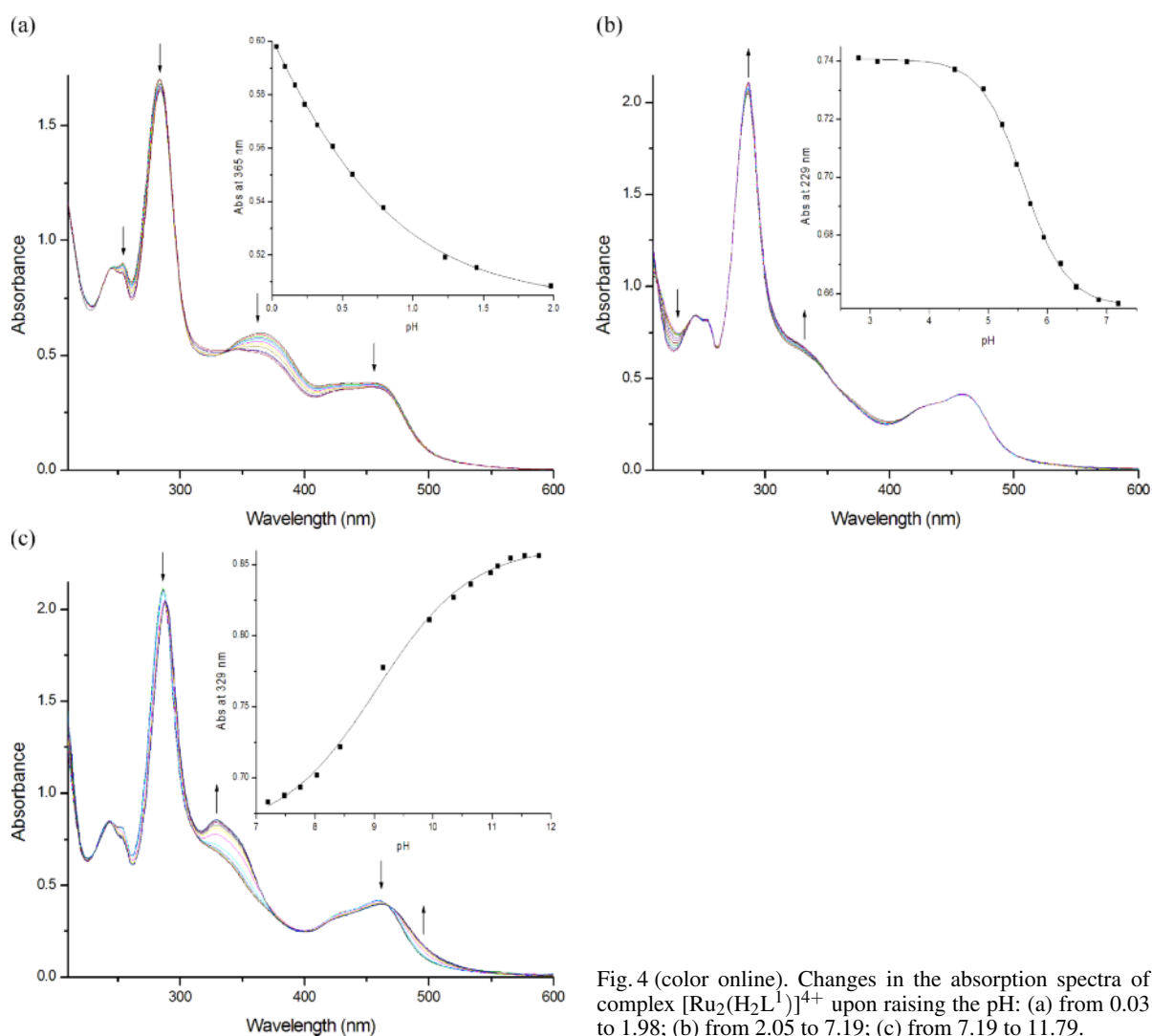


Fig. 4 (color online). Changes in the absorption spectra of complex $[\text{Ru}_2(\text{H}_2\text{L}^1)]^{4+}$ upon raising the pH: (a) from 0.03 to 1.98; (b) from 2.05 to 7.19; (c) from 7.19 to 11.79.

As the pH increases from 0.03 to 1.98, the fluorescence intensity increases by about 39% (Fig. 5a). Hence, complex $[\text{Ru}_2(\text{H}_2\text{L}^1)]^{4+}$ acts as an “off-on” fluorescence pH switch during the process. When the pH is increased from 2.05 to 7.19, the emission maxima are blue-shifted from 624 to 613 nm, and the emission intensities decrease by about 27% (Fig. 5b). The fluorescence of the complex is partly quenched because the protonated bridging ligand is a better π acceptor than the peripheral 2,2'-bipyridine ligands [38]. On further raising the pH from 7.19 to 11.79 (Fig. 5c), the emission intensities are found to decrease sharply by about 87%, and the emission maxima are red-shifted from 613 to 625 nm. Especially over the pH range from 8.03 to 9.15, the complex $[\text{Ru}_2(\text{H}_2\text{L}^1)]^{4+}$ shows obvious variations in the emission spectra with a maximum

on-off ratio of 6. This on-off ratio compares favorable with the data reported for analogous imidazole-containing Ru(II) polypyridyl complexes [20–22]. Hence, $[\text{Ru}_2(\text{H}_2\text{L}^1)]^{4+}$ acts as an effective “on-off” fluorescence pH switch over the stated pH range. This behavior may involve rapid radiationless decay [32]. It has been well documented that the energy of metal-centered excited states depends on the prevailing ligand field strength, which in turn depends on the σ -donor and π -acceptor properties of the ligand. The negative charge on the deprotonated imidazole rings can be delocalized over the whole π framework, decreasing the σ -donor and increasing the π -acceptor capacity of the bridging ligand, and resulting in a weakening of the ligand field strength around the metal center and in turn lowering the metal σ^* orbitals [20–22]. The

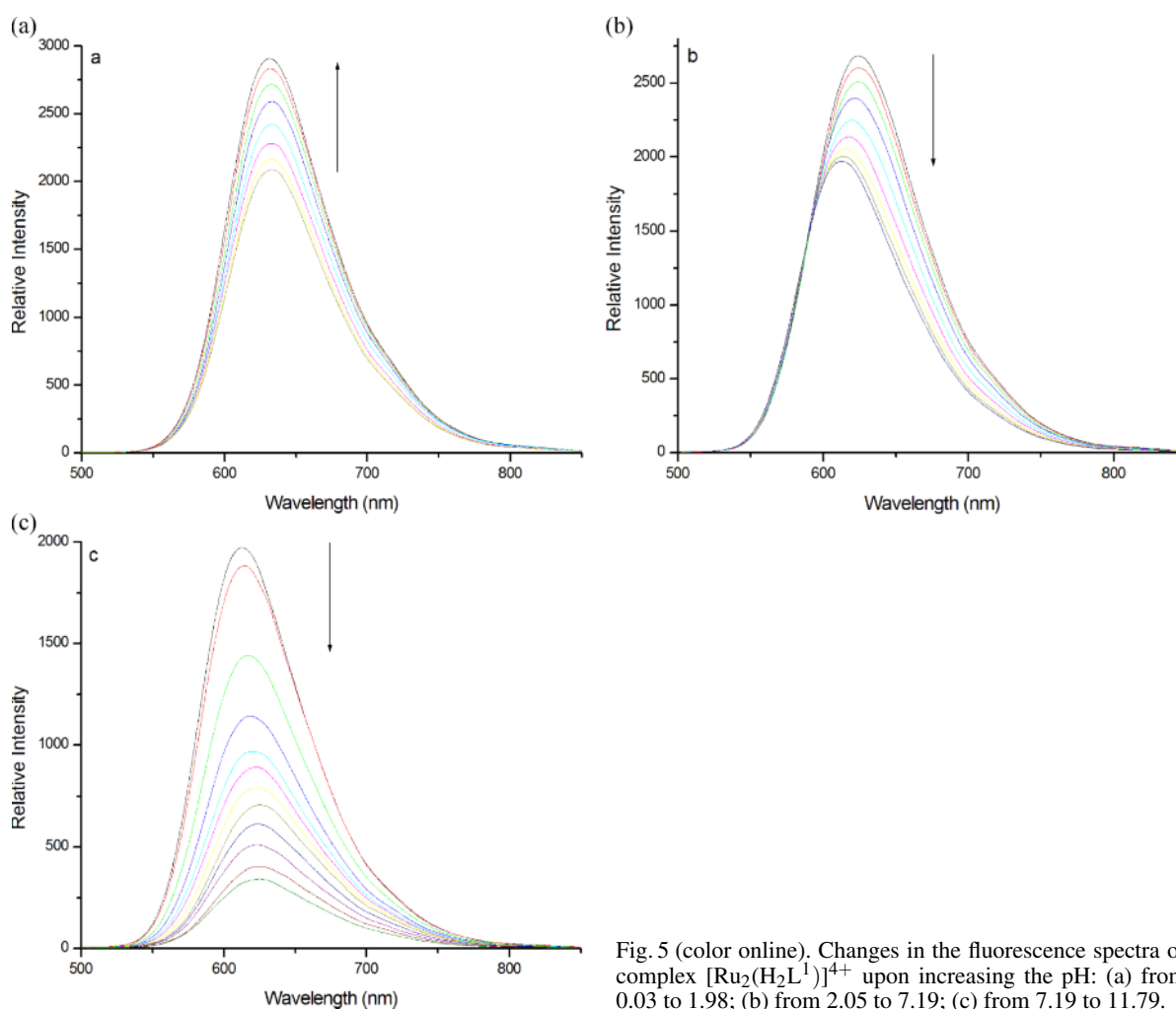


Fig. 5 (color online). Changes in the fluorescence spectra of complex $[\text{Ru}_2(\text{H}_2\text{L}^1)]^{4+}$ upon increasing the pH: (a) from 0.03 to 1.98; (b) from 2.05 to 7.19; (c) from 7.19 to 11.79.

value of ΔE between the metal σ^* orbital and metal π orbital of the deprotonated complex $[\text{Ru}_2(\text{L}^1)]^{2+}$ is lower than that of the complex $[\text{Ru}_2(\text{H}_2\text{L}^1)]^{4+}$. Consequently, population of the excited state is very efficient for the deprotonated complex, and this complex is essentially weakly emissive at room temperature. The excited state ionization constant $\text{p}K_{\text{a}}^*$ could be estimated on the basis of the Förster cycle [36], which correlates $\text{p}K_{\text{a}}^*$ with $\text{p}K_{\text{a}}$ thermodynamically by the equation $\text{p}K_{\text{a}}^* = \text{p}K_{\text{a}} + (0.625/T)(\nu_{\text{B}} - \nu_{\text{HB}})$, in which ν_{B} and ν_{HB} are pure 0–0 transitions in cm^{-1} for the basic and acidic species, respectively. In practice, ν_{B} and ν_{HB} are often difficult or even impossible to obtain. A good approximation is to use the emission maxima for ν_{B} and ν_{HB} since a protonation equilibrium is almost certainly established between the $^3\text{MLCT}$ states [41]. Therefore, the energies of the emission maxima in wavenumbers are used in the equation, giving three excited state ionization constants of $\text{p}K_{\text{a}1}^* = 1.43$, $\text{p}K_{\text{a}2}^* = 5.31$, and $\text{p}K_{\text{a}3}^* = 9.36$. The value of $\text{p}K_{\text{a}3}^*$ is 0.30 $\text{p}K_{\text{a}}$ units greater than the value of $\text{p}K_{\text{a}3}$, indicating that the electron density of the excited state is higher than that of the ground state, and the excited electron is directed to the H_2L^1 rather than to the 2,2'-bipyridine ligand. The increase in electron density on the ligand H_2L^1 increases its basicity and, therefore, increases the excited state $\text{p}K_{\text{a}}^*$ value.

The spectroscopic properties of the complex $[\text{Ru}(\text{HL}^2)]^{2+}$ are similar to those of $[\text{Ru}_2(\text{H}_2\text{L}^1)]^{4+}$. $[\text{Ru}(\text{HL}^2)]^{2+}$ also undergoes three successive deprotonation processes. The values of the three ground-state ionization constants $\text{p}K_{\text{a}1}$, $\text{p}K_{\text{a}2}$, and $\text{p}K_{\text{a}3}$ are 2.08, 5.32, and 9.02, and the values of the three excited state ionization constants $\text{p}K_{\text{a}1}^*$, $\text{p}K_{\text{a}2}^*$, and $\text{p}K_{\text{a}3}^*$ are 2.10, 5.07, and 9.37, respectively.

Conclusion

Two polypyridyl ligands and their Ru(II) complexes containing uncoordinated imidazole rings along with piperazine or morpholine rings have been prepared and characterized. Both complexes have a broad pH-sensing range, and the photophysical properties of both complexes are strongly dependent on the pH value of the solution. Both complexes act as “off-on-off” fluorescence pH sensors, with a maximum on-off ratio of 6. The two complexes have potential utility to detect pH changes in the environment, due to their proton-dependent fluorescence properties.

Acknowledgement

We are grateful to the Yunnan provincial science and technology department (2010ZC148) and Shanghai key laboratory of rare earth functional materials for financial support.

- [1] K. J. Herbst, M. D. Allen, J. Zhang, *J. Am. Chem. Soc.* **2011**, *133*, 5676–5679.
- [2] R. S. Sánchez, R. Gras-Charles, J. L. Bourdelande, G. Guirado, J. Hernando, *J. Phys. Chem. C* **2012**, *116*, 7164–7172.
- [3] J. R. Siekierzycka, C. Hippus, F. Würthner, R. M. Williams, A. M. Brouwer, *J. Am. Chem. Soc.* **2010**, *132*, 1240–1242.
- [4] B. R. Spencer, B. J. Kraft, C. G. Hughes, M. Pink, J. M. Zaleski, *Inorg. Chem.* **2010**, *49*, 11333–11345.
- [5] A. Praetorius, D. M. Bailey, T. Schwarzlose, W. M. Nau, *Org. Lett.* **2008**, *10*, 4089–4092.
- [6] C. Zhou, Y. Li, Y. Zhao, J. Zhang, W. Yang, Y. Li, *Org. Lett.* **2011**, *13*, 292–295.
- [7] R. S. Sánchez, R. Gras-Charles, J. L. Bourdelande, G. Guirado, J. Hernando, *Org. Lett.* **2011**, *13*, 5572–5575.
- [8] P. Bandyopadhyay, A. K. Ghosh, *J. Phys. Chem. B* **2009**, *113*, 13462–13464.
- [9] A. S. Stepanov, V. V. Yanilkin, A. R. Mustafina, V. A. Burilov, S. S. Solovieva, I. Antipin, A. I. Konovalov, *Electrochem. Commun.* **2010**, *12*, 703–705.
- [10] Q. M. Wang, K. Ogawa, K. Toma, H. Tamiaki, *J. Photochem. Photobiol. A* **2009**, *201*, 87–90.
- [11] K. Seo, A. V. Konchenko, J. Lee, G. S. Bang, H. Lee, *J. Am. Chem. Soc.* **2008**, *130*, 2553–2559.
- [12] D. J. Stewart, P. E. Fanwick, D. R. McMillin, *Inorg. Chem.* **2010**, *49*, 6814–6816.
- [13] D. A. Jose, P. Kar, D. Koley, B. Ganguly, W. Thiel, H. N. Ghosh, A. Das, *Inorg. Chem.* **2007**, *46*, 5576–5584.
- [14] H. M. R. Gonçalves, C. D. Maule, P. A. S. Jorge, J. C. G. Esteves da Silva, *Anal. Chim. Acta* **2008**, *626*, 62–70.
- [15] Y. Pellegrin, R. J. Forster, T. E. Keyes, *Inorg. Chim. Acta* **2009**, *362*, 1715–1722.
- [16] L. Herman, B. Elias, F. Pierard, C. Moucheron, A. K. Mesmaeker, *J. Phys. Chem. A* **2007**, *111*, 9756–9763.
- [17] T. Ayers, N. Caylor, G. Ayers, C. Godwin, D. J. Hathcock, V. Stuman, S. J. Slattery, *Inorg. Chim. Acta* **2002**, *328*, 33–38.
- [18] M. Haga, T. Takasugi, A. Tomie, M. Ishizuya, T. Yamada, *J. Chem. Soc., Dalton Trans.* **2003**, 2069–2079.

- [19] S. Baitalik, U. Flörke, K. Nag, *J. Chem. Soc., Dalton Trans.* **1999**, 719–728.
- [20] A. Quaranta, F. Lachaud, C. Herrero, R. Guillot, M. F. Charlot, W. Leibl, A. Aukauloo, *Chem. Eur. J.* **2007**, *13*, 8201–8211.
- [21] S. H. Fan, A. G. Zhang, C. C. Ju, L. H. Gao, K. Z. Wang, *Inorg. Chem.* **2010**, *49*, 3752–3763.
- [22] F. Gao, X. Chen, F. Zhou, L. P. Weng, L. T. Guo, M. Chen, H. Chao, L. N. Ji, *Inorg. Chim. Acta* **2011**, *370*, 132–140.
- [23] C. Hiort, P. Lincoln, B. Norden, *J. Am. Chem. Soc.* **1993**, *115*, 3448–3454.
- [24] W. H. N. Nijhuis, W. Verboom, D. F. Reinhoudt, *Synthesis* **1987**, *7*, 641–645.
- [25] B. P. Sullivan, D. J. Salmon, T. J. Meyer, *Inorg. Chem.* **1978**, *17*, 3334–3341.
- [26] E. A. Steck, A. R. Day, *J. Am. Chem. Soc.* **1943**, *65*, 452–456.
- [27] S. Maji, B. Sarkar, M. Patra, A. K. Das, S. M. Mobin, W. Kaim, G. K. Lahiri, *Inorg. Chem.* **2008**, *47*, 3218–3227.
- [28] D. P. Rillema, K. B. Mack, *Inorg. Chem.* **1982**, *21*, 3849–3854.
- [29] R. J. Watts, G. A. Crosby, *J. Am. Chem. Soc.* **1972**, *94*, 2606–2614.
- [30] E. M. Kober, J. L. Marshall, W. J. Dressick, B. P. Sullivan, J. V. Caspar, T. J. Meyer, *Inorg. Chem.* **1985**, *24*, 2755–2763.
- [31] E. Amouyal, A. Homsy, J. C. Chambron, J. P. Sauvage, *J. Chem. Soc., Dalton Trans.* **1990**, 1841–1845.
- [32] A. Juris, V. Balzani, F. Barigelletti, S. Campagna, P. Belser, A. von Zelewsky, *Coord. Chem. Rev.* **1988**, *84*, 85–277.
- [33] Z. J. Jia, T. Ramstad, M. Zhong, *Electrophoresis* **2001**, *22*, 1112–1118.
- [34] N. R. De Tacconi, R. O. Lezna, R. Konduri, F. Ongeri, K. Rajeshwar, F. M. MacDonnell, *Chem. Eur. J.* **2005**, *11*, 4327–4339.
- [35] T. N. Brown, N. Mora-Diez, *J. Phys. Chem. B* **2006**, *110*, 20546–20554.
- [36] B. Knobloch, H. Sigel, A. Okruszek, R. K. O. Sigel, *Org. Biomol. Chem.* **2006**, *4*, 1085–1090.
- [37] K. O'Donoghue, J. C. Penedo, J. M. Kelly, P. E. Kruger, *J. Chem. Soc., Dalton Trans.* **2005**, 1123–1128.
- [38] R. Grigg, W. D. J. A. Norbert, *J. Chem. Soc., Dalton Trans.* **1992**, 1300–1302.
- [39] M. J. Han, L. H. Guo, Y. Y. Lu, K. Z. Wang, *J. Phys. Chem. B* **2006**, *110*, 2364–2371.
- [40] H. Chao, B. H. Ye, H. Li, R. H. Li, J. Y. Zhou, L. N. Ji, *Polyhedron* **2000**, *19*, 1975–1983.
- [41] G. Y. Zheng, Y. Wang, D. P. Rillema, *Inorg. Chem.* **1996**, *35*, 7118–7123.